Supporting Information

Lamellar Crystal-Dominated Surface of Polymer Film Achieved by Melt Stretching-Induced Free Surface Crystallization

Xiaohui Wang[a], Feifei Yan[a], Xue Bai[a], Hanchuan Li[a], Ming Yuan[a], Yanping Liu[b,*], Benjamin S. Hsiao[c], Chuntai Liu[a], Zhen Wang[a,*]

[a]*National Engineering Research Center for Advanced Polymer Processing Technology, Key Laboratory of Materials Processing and Mold (Zhengzhou University), Ministry of Education, Zhengzhou University, Zhengzhou, 450002, China*

[b]*National Center for International Research of Micro-nano Molding Technology & Key Laboratory for Micro Molding Technology of Henan Province, Zhengzhou University, Zhengzhou 450002, China*

[c]*Department of Chemistry, Stony Brook University, Stony Brook, NY, 11794-3400, USA*

[*]Corresponding authors: ypliu@zzu.edu.cn; wangz@zzu.edu.cn

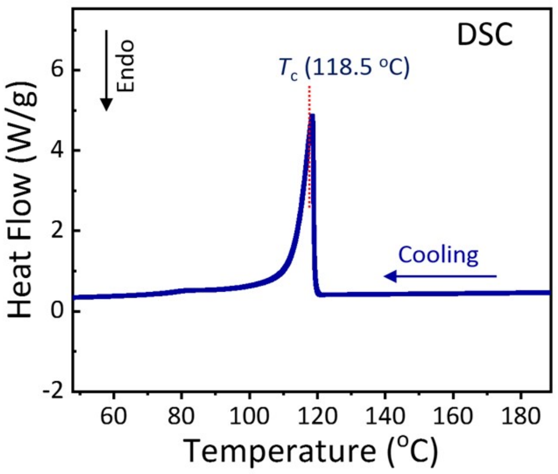

Fig. S1 DSC curve upon cooling at a rate of 10 °C/min for the raw PE. The exothermic peak of crystallization is at about 118.5 °C (T_c). Thus the melt stretching temperature of 130 °C is between the T_c and the equilibrium melting temperature (T_m^o, 141.4 °C),[1] corresponding to a supercooled state of PE melt.

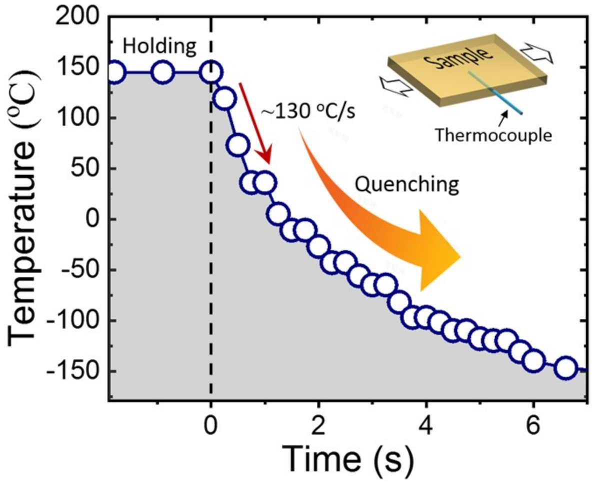

Fig. S2 Cooling profile during quenching the melt measured by inserting a thermocouple probe in the inside of sample. It is seen that the quenching operation with liquid nitrogen achieves an average cooling rate of about 130 °C/s from 150 to 50 °C.

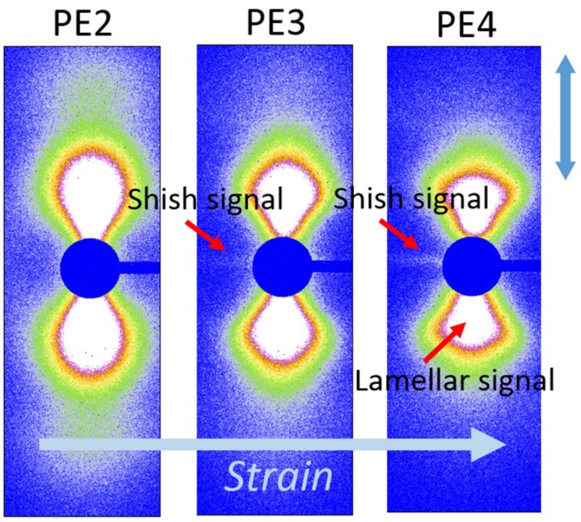

Fig. S3 2D SAXS patterns of PE2, PE3 and PE4. Due to the whole film thickness larger than 250 μm, the scattering signal from thin surface layer (thickness, < 1 μm) is negligible. The SAXS patterns are mainly determined by the crystal structure in the bulk film. With increasing the strain to above 3, there is a streak scattering appearing perpendicular to the melt stretching direction. Such a signal has been suggested to come from the rod-like shish entities that are usually formed under strong flow field.[2] While for the strain below 2, only lamellar scattering can be observed, indicating the lack of shish. These SAXS results are consistent with the direct SEM observation in Fig. 2.

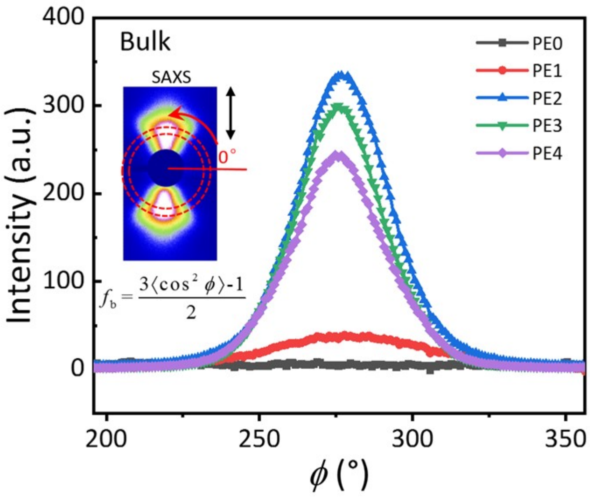

Fig. S4 Intensity distribution of SAXS patterns along the azimuthal angle from 180 to 360^{o} for different kinds of PE films. The insertion shows the integral region (q range of 0.20~0.25 nm^{-1}) in the 2D SAXS patterns. Along with increasing the strain, the lamellar scattering concentrates gradually on the melt stretching direction, causing a sharp peak of azimuthal intensity distribution. This denotes the formation of highly oriented lamellae in the bulk film.

Calculation method of lamellar orientational parameter. To evaluate the lamellar orientation, the intensity distribution curves against azimuthal angle are obtained from 2D SAXS and FFT patterns (Fig. S4 and 5). Lamellar orientational degree (f) is quantified using the Herman's orientational parameter, which is the ensemble average of the second Legendre polynomial[3]

$$f=\frac{3\langle\cos^2\phi\rangle\text{-}1}{2}$$

where ϕ is the azimuthal angle. $\langle\cos^2\phi\rangle$ is attained from the azimuthal scattering intensity distribution by

$$\langle\cos^2\phi\rangle=\frac{\int_0^{\pi/2} I(\phi)\sin\phi\langle\cos^2\phi\rangle d\phi}{\int_0^{\pi/2} I(\phi)\sin\phi d\phi}$$

where $I(\phi)$ is the scattering intensity at azimuth of ϕ. The f is 0 when the lamellae are isotropically distributed and 1 when the lamellae are in perfect alignment parallel to the melt stretching direction.

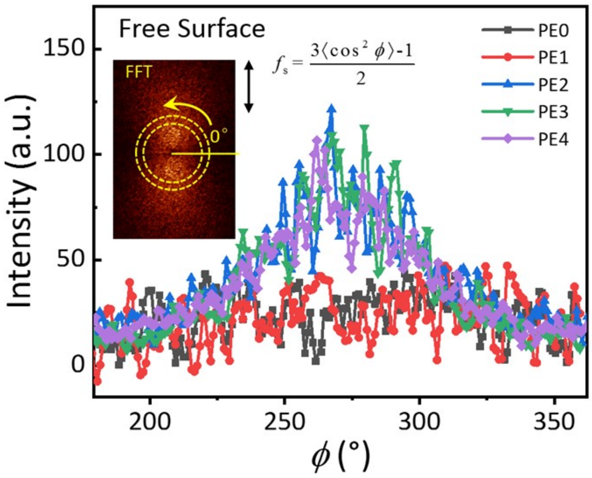

Fig. S5 Intensity distribution of FFT scattering patterns along the azimuthal angle from 180 to 360 ^{o}C for different kinds of PE films. The insertion shows the integral region (*k* range of 0.002~0.004 nm^{-1}) in the 2D FFT patterns. It is found that increasing the strain leads to a concentration of lamellar scattering on the melt stretching direction, denoting an enhancement of lamellar orientation. However, compared to the SAXS (Fig. S4), the intensity peak of FFT is much blunter. This indicates that the free surface adopts a lamellar orientation much lower than the bulk under the same flow condition. Note that the surface lamellar orientation is quantified also by employing the Herman's orientational parameter.

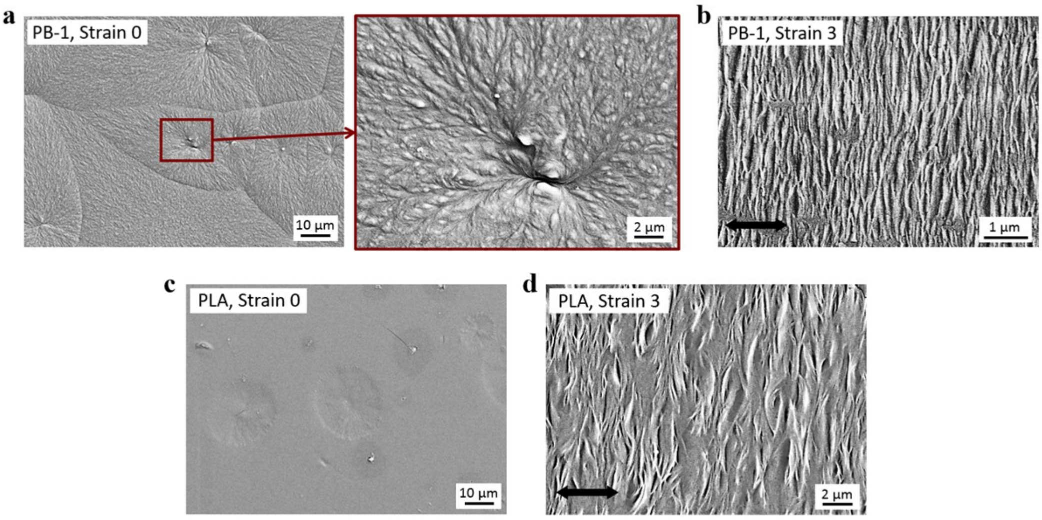

Fig. S6 SEM images of the free surface of PB-1 films prepared by melt stretching with strains of 0 (a) and 3 (b) and PLA films prepared by melt stretching with strains of 0 (c) and 3 (d).

Constructing the lamellar crystal-dominated (LCD) surface of polybutene-1 (PB-1) and polylactic acid (PLA) films. We have checked the applicability of melt stretching-induced free surface crystallization in constructing the LCD surface of PB-1 and PLA films. The overall experimental procedures are the same as that of PE except for the melt stretching temperature (T_s). The T_s is 120 °C for PB-1 (supercooled melt), while 140 °C for PLA (supercooled melt). Fig. S6a-d show the SEM images of the free surface of PB-1 and PLA films. We can see that the static melt crystallization without flow leads to the film surface of PB-1 covered by large-scale spherulites (Fig. S6a), where many protuberances are radially distributed about the spherulite center. When imposing the melt stretching with strain of 3, regular lamellar morphology is formed (Fig. S6b). This result is similar with the experimental observation of PE, even though the lamellar orientation of PB-1 seems stronger. For PLA, due to a kinetically slow nature of crystallization,[4] only sporadically distributed spherulites are identified on the film surface under static condition (Fig. S6c). When the melt is stretched to strain of 3, the orientated lamellar alignment can be seen (Fig. S6d). However, the lamellar structure covers only partial region of film surface and the rest is amorphous phase. The reason for this may be related to the molecular parameter or the melt stretching condition, which will be studied in the future work. In general, we have confirmed that the crystallization-driven formation of LCD surface is also valid for PB-1 and PLA, although the detailed morphologies show some differences from PE. Since the free surface effects are immanent to existence in polymer materials, the currently proposed melt processing strategy is transferable to other semicrystalline polymers.

References

1 B. Wunderlich and G. Czornyj, *Macromolecules*, 1977, **10**, 906-913.

2 T. Yan, B. Zhao, Y. Cong, Y. Fang, S. Cheng, L. Li, G. Pan, Z. Wang, X. Li and F. Bian, *Macromolecules*, 2010, **43**, 602-605.

3 J. L. White and J. E. Spruiell, *Polym. Eng. Sci.*, 1983, **23**, 247-256.

4 S. Saeidlou, M. A. Huneault, H. Li and C. B. Park, *Prog. Polym. Sci.*, 2012, **37**, 1657-1677.